Realistic nucleon-nucleon interactions and the three-body electrodisintegration of ^{3}H

C. Ciofi degli Atti
Istituto Nazionale di Fisica Nucleare, Sezione Sanità, Rome, Italy
and Radiation Laboratory, Istituto Superiore di Sanità, Rome, Italy

E. Pace
Istituto Nazionale di Fisica Nucleare, Sezione Sanità, Rome, Italy
and Istituto di Fisica, Università di Roma, Rome, Italy

G. Salmè
Istituto Nazionale di Fisica Nucleare, Sezione Sanità, Rome, Italy
and Radiation Laboratory, Istituto Superiore di Sanità, Rome, Italy
(Received 8 June 1979)

The three-body variational wave functions resulting from two realistic nucleon-nucleon interactions featuring different deuteron D-wave probabilities have been used in the calculation of the three-body electrodisintegration of triton in the quasi-elastic region. The angular distributions of the coincidence cross section ^{3}H$(e,e'p)2n$ are found to depend sensitively upon the D-wave probability in the triton. In the case of the Reid soft core interaction a comparison of the $T = 1$ spectral functions corresponding to the Faddeev and variational wave functions reveals an appreciably larger high momentum content in the latter.

[NUCLEAR REACTIONS ^{3}H$(e,e'p)$ $2n$, calculated spectral function $P(k, E_2)$, angular distributions of coincidence process, quasi-elastic peak, energy-weighted sum rule. Three-body variational wave functions; Reid and RHEL-1 nucleon-nucleon interactions.]

I. INTRODUCTION

The development of accurate computational techniques[1-5] has made it possible in recent years to obtain the solution of the three-body nonrelativistic Schrödinger equation corresponding to realistic interactions with a high degree of reliability. The validity of the three-body wave function has been investigated by calculating such quantities as the binding energy, the rms charge radii, and the charge form factor (extensive reviews on the three-body problem in nuclear physics are given in Refs. 6–9). Recently, in order to investigate in more detail the structure of the three-body wave function, the photodisintegration process and the quasi-elastic electron scattering on ^{3}He have also been studied. The photodisintegration of ^{3}He at low and intermediate energies has been analyzed by Craver *et al.*[10] using the wave function obtained by Brandenburg *et al.*[1a] from the momentum space Faddeev formalism developed by Harper *et al.*[1c] and corresponding to the Reid soft core (RSC) potential.[11] The same wave function has been used by Dieperink *et al.*[12] in the calculation of the quasi-elastic electron scattering by ^{3}He obtaining, unlike the case of Tabakin's interaction, a satisfactory explanation of the experimental data, except for the high energy transfer tail and the top of the peak. In a previous paper[13] we have pointed out that, in order to have a more complete understanding of the merits and the drawbacks of realistic nonrelativistic three-body wave functions, it would be very useful to analyze various scattering processes in terms of three-body wave functions different from those used in Refs. 10 and 12. In Ref. 13 preliminary results concerning the calculation of the three-body electrodisintegration of ^{3}H performed with the variational wave function of Nunberg *et al.*[4] were reported. In the present paper the calculations of Ref. 13 are extended in three respects: (1) The calculation with the RSC interaction is completed. (2) The wave function[4b] resulting from another realistic interaction, viz. the RHEL-1 interaction,[14] is also used. (3) The binding energy per proton E_z/Z has been calculated using the energy-weighted sum rule.[15]

Our paper is organized as follows: In Sec. II the structure of the three-body wave function and the main features of the two-nucleon potentials considered are recalled. In Sec. III the calculated proton spectral function for the three-body electrodisintegration of ^{3}H is presented and a comparison is made with the corresponding quantity obtained from the Faddeev wave function of Ref. 1(a); moreover, the sensitivity of the spectral function upon the structure of the triton wave function and the spectator pair final-state interaction is discussed. In Secs. IV and V, respectively, the re-

sults of the calculation of the coincidence cross section of the $^3H(e,e'p)2n$ reaction and of the contribution of this process to the quasi-elastic peak are presented. In Sec. VI the energy-weighted sum rule is calculated and, finally, in Sec. VII the results are discussed and the conclusions are drawn.

The study of electrodisintegration and photodisintegration processes with the variational wave function of Ref. 4 is of particular relevance in light of the recent results on the calculation of elastic electron scattering by ^3He and ^3H performed in Refs. 16 and 17. There it has been found that the charge form factor and the charge point density of ^3He appreciably differ from the corresponding quantities obtained using the Faddeev wave functions of Refs. 1, 2, and 18.

Our calculations of the electrodisintegration of ^3H are the first ones performed using three-body wave functions corresponding to realistic nucleon-nucleon interactions. A calculation of the coincidence cross section and the quasi-elastic peak was previously performed by Lehman[19] who, however, used a simple S-wave separable interaction.

II. THE NUCLEON-NUCLEON INTERACTION AND THE TRITON WAVE FUNCTION

The triton wave functions used in this work have been obtained by diagonalizing the nonrelativistic intrinsic Hamiltonian

$$H=\sum_{i=1}^{3}\frac{p_i^2}{2M}-T_{\text{c.m.}}+\sum_{1=i<j}^{3}v(i,j)\,, \tag{1}$$

where M is the nucleon mass and

$$T_{\text{c.m.}}=\left(\sum_{i=1}^{3}\vec{p}_i\right)^2\Big/\,6M$$

the kinetic energy operator associated with the center of mass motion.

(a) *Nucleon-nucleon interaction.* Two different nucleon-nucleon potentials $v(i,j)$ have been used in Eq. (1), namely

(i) the RSC interaction which, as is well known, is defined for waves with angular momentum $J\leq 2$,

(ii) the Rutherford-High-Energy-Laboratory potential, developed by Ulehla[14] (RHEL-1 potential), which is a potential with a slightly softer short range repulsion than the one of the RSC interaction yielding a very good fit of the experimental phase shifts. The RHEL-1 potential is defined in all waves with angular momentum $J\leq 5$ and $l<6$. However, in Ref. 4 only the waves with $l\leq 4$ have been considered.

The above interactions mainly differ in the predicted D wave probability in deuteron ($P_D^{\text{RSC}}=6.47\%$ and $P_D^{\text{RHEL-1}}=4.7\%$, respectively), resulting in different values for the binding energy and D wave probability of triton (see Table I).

TABLE I. Binding energy E_3, rms charge radius $\langle r^2\rangle^{1/2}$ and percentage of the various waves in ^3H, calculated with the RSC (Ref. 11) and RHEL-1 (Ref. 14) interactions (Ref. 4). Note that the values for E_3 and $\langle r^2\rangle^{1/2}$ are extrapolated values, whereas the values for P_L correspond to $Q_{\text{max}}=28$.

	RSC	RHEL-1	Exp
E_3(MeV)	-7.3 ± 0.2	-8.1 ± 0.2	-8.48
$\langle r^2\rangle^{1/2}$ (fm)	1.85	1.79	1.70 ± 0.05
$P_{S+S'}$ (%)	89.9	92.34	
P_D (%)	10.0	7.6	
P_P (%)	0.1	0.06	

(b) *Triton wave function.* The diagonalization of the Hamiltonian (1) has been performed by expanding the triton wave function $|\psi^{\mu}_{1/2}\rangle$ in an intrinsic harmonic oscillator basis depending upon the intrinsic variables

$$\vec{a}=\frac{1}{\sqrt{2}}(\vec{r}_1-\vec{r}_2)\,,$$
$$\vec{b}=\frac{1}{\sqrt{2}}[2\vec{r}_3-(\vec{r}_1+\vec{r}_2)]\,, \tag{2}$$

where the subscripts 1 and 2 label the like particles (neutrons) and the subscript 3 the unlike particle (proton). In Ref. 4 the isospin formalism has not been used, so that the wave function is written in the following form:

$$|\psi^{\mu}_{1/2}\rangle=\sum_i C_i\sum_{\substack{m_a m_b\\ M_L M_S}}\langle l_a m_a l_b m_b|LM_L\rangle \times\langle LM_L\,SM_S|\tfrac{1}{2}\mu\rangle\,|n_a l_a m_a\rangle_{\rho_a} \times|n_b l_b m_b\rangle_{\rho_b}|S_{12}\tfrac{1}{2};SM_S\rangle\,, \tag{3}$$

where $i\equiv\{n_a,l_a,n_b,l_b,L,S_{12},S\}$, $|n_a l_a m_a\rangle_{\rho_a}$ and $|n_b l_b m_b\rangle_{\rho_b}$ are two harmonic oscillator wave functions with oscillator parameters ρ_a and ρ_b [$\rho=(\hbar/M\omega)^{1/2}$], $|S_{12}\,\frac{1}{2};SM_S\rangle$ is the three-body spin function, and L, S, and $J=\frac{1}{2}$ are, respectively, the triton orbital, spin, and total angular momenta (cf. Fig. 1).

The diagonalization of the Hamiltonian (1) is carried out by increasing the maximum number Q_{max} of oscillator quanta $Q=2n_a+l_a+2n_b+l_b$ included in the basis, until the convergence of the binding energy E_3 is reached. Thanks to the introduction of two nonlinear variational parameters ρ_a and ρ_b, a good convergence of the binding energy is achieved already for $Q_{\text{max}}=28$. (The details of this procedure are described in Refs. 4 and 17, therefore, they will not be repeated here where

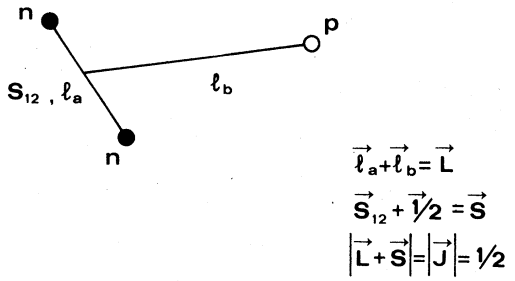

FIG. 1. Coordinates and angular momenta used in the wave function [Eq. (3)].

only the final results pertaining to various observables of ^{3}H are listed in Table I.) It should be pointed out that when this type of wave function is used it is always necessary to check the convergence of the expectation value of any operator as $Q_{\max}$ increases. It has been shown[17] that the charge form factor of ^{3}He converges very well for $Q_{\max}=28$ even at very large values of the momentum transfer. The convergence of the cross sections considered in this paper will be discussed at the proper place.

III. THE PROTON SPECTRAL FUNCTION IN THE THREE-BODY ELECTRODISINTEGRATION OF TRITON

The process we are going to consider is the three-body electrodisintegration of ^{3}H

$$e+{}^3\mathrm{H}\rightarrow e'+p+(nn)\,, \tag{4}$$

which is supposed to occur by a direct collision of the incoming electron with four-momentum $k_{1\mu}\equiv\{\vec{k}_1, i\epsilon_1\}$ with a bound proton moving, after interaction, with asymptotic four-momentum $k_{p\mu}\equiv\{\vec{k}_p, i\epsilon_p\}$; the four momentum of the scattered electron will be $k_{2\mu}\equiv\{\vec{k}_2, i\epsilon_2\}$, the center of mass recoil momentum of the neutron-neutron (nn) pair $k_{R\mu}\equiv\{\vec{k}_R, i\epsilon_R\}$ and the relative momentum and energy of the pair $\vec{t}$ and t^2/M, respectively. We use the ultrarelativistic approximation for the electrons, i.e., $m_e=0$, $|\vec{k}|=\epsilon$, and a metric such that

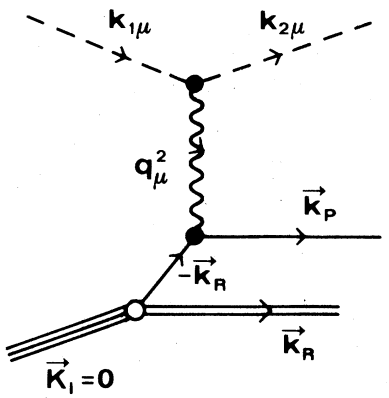

FIG. 2. One-photon-exchange diagram for the process $^3\mathrm{H}(e,e'p)2n$.

the four-momentum transfer is $q_\mu{}^2=\vec{q}^2-\omega^2$, where $\vec{q}=\vec{k}_1-\vec{k}_2$ and $\omega=\epsilon_1-\epsilon_2$; furthermore, the proton and the recoiling-pair motions will be treated nonrelativistically. The momentum and energy conservation will therefore be expressed by the equations

$$\vec{q}=\vec{k}_p+\vec{k}_R\,, \tag{5}$$

$$\omega=\frac{k_p{}^2}{2M}+\frac{(\vec{q}-\vec{k}_p)^2}{4M}+|E_3|+\frac{t^2}{M}\,, \tag{6}$$

where $T_p=k_p{}^2/2M$ is the kinetic energy of the emitted proton, $(\vec{q}-\vec{k}_p)^2/4M$ the recoil energy of the neutron pair, and $|E_3|=M_p+2M_n-M_3$, with $|E_3|$ being the calculated binding energy of triton.

Two main approximations have been used in the derivation of the cross section for the process (4), namely (i) the one-photon-exchange approximation for the electron-nucleus interaction, and (ii) the plane-wave approximation (PWA) for the emitted nucleon. The limits of validity of the PWA will be discussed later on.

The cross section for the process (4), shown diagrammatically in Fig. 2, has the following form[13]:

$$\frac{d^8\sigma}{dk_p d\Omega_p d\epsilon_2 d\Omega_2 dk_R d\Omega_R dt\, d\Omega_t}=(2\pi)^4\delta^3(\vec{q}-\vec{k}_p-\vec{k}_R)\delta[\omega-|E_3|-k_p{}^2/2M-(\vec{q}-\vec{k}_p)^2/4M-t^2/M]$$

$$\times\tfrac{1}{2}\sum_{\substack{\sigma_p\mu\\ S_f M_f}}\tfrac{1}{2}\sum_{\sigma_1,\sigma_2}\left|\langle\psi^{\vec{t}}_{S_f M_f}\chi_{\vec{k}_p\sigma_p}\varphi_{\vec{k}_2\sigma_2}|H|\psi^{\mu}_{1/2}\varphi_{\vec{k}_1\sigma_1}\rangle\right|^2\frac{k_p{}^2}{(2\pi)^3}\frac{\epsilon_2{}^2}{(2\pi)^3}\frac{k_R{}^2}{(2\pi)^3}\frac{t^2}{(2\pi)^3}\,, \tag{7}$$

where $\psi^{\vec{t}}_{S_f M_f}$ is the two-body final state wave function, $\chi_{\vec{k}_p\sigma_p}$ is the emitted proton wave function, and $\varphi_{\vec{k}\sigma}$ is the electron plane wave. Using the nonrelativistic reduction of the electron-proton interaction and retaining terms up to order $(q/M)^2$ (see, e.g., Ref. 20), summing over electron spin projection and integrating over $\vec{k}_R$ and the direction of $\vec{t}$, one obtains

$$\frac{d^5\sigma}{dE_2 d\epsilon_2 d\Omega_2 dT_p d\Omega_p} = k_p\, M(d\sigma/d\Omega)_{ep}\, P(k, E_2)\delta\left(\omega - |E_3| - \frac{k_p^2}{2M} - \frac{(\vec{q}-\vec{k}_p)^2}{4M} - \frac{t^2}{M}\right), \tag{8}$$

where

$$\vec{k} = -\vec{k}_R = \vec{k}_p - \vec{q} \tag{9}$$

is the momentum of the bound proton,

$$E_2 = t^2/M \tag{10}$$

is the energy of the neutron pair,

$$\left(\frac{d\sigma}{d\sigma}\right)_{ep} = \sigma_{\text{Mott}}\left\{\bar{G}_E^p(q_\mu{}^2)^2\left[1 + \frac{1}{4M^2}\, tg^2\frac{\theta}{2}\,(2\vec{k}_p - \vec{q})^2 - \frac{1}{2M}\sec^2\frac{\theta}{2}\,[\hat{k}_1\cdot(2\vec{k}_p - \vec{q}) + \hat{k}_2\cdot(2\vec{k}_p - \vec{q})]\right.\right.$$
$$\left.\left. + \frac{1}{4M^2}\sec^2\frac{\theta}{2}\,\hat{k}_2\cdot(2\vec{k}_p - \vec{q})\hat{k}_1\cdot(2\vec{k}_p - \vec{q})\right] + \bar{G}_M^p(q_\mu{}^2)^2\,\frac{q^2}{4M^2}\left(1 + 2\,tg^2\frac{\theta}{2}\right)\right\} \tag{11}$$

is the electron-proton cross section defined in terms of the Mott cross section ($\alpha = 1/137$)

$$\sigma_{\text{Mott}} = \frac{\alpha^2}{4\epsilon_1^2}\frac{\cos^2(\theta/2)}{\sin^4(\theta/2)}, \tag{12}$$

and the generalized Sachs form factors

$$\bar{G}_E^p(q_\mu{}^2) = \frac{G_E^p(q_\mu{}^2)}{(1 + q_\mu{}^2/4M^2)^{1/2}}, \quad \bar{G}_M^p(q_\mu{}^2) = \frac{G_M^p(q_\mu{}^2)}{(1 + q_\mu{}^2/4M^2)^{1/2}}. \tag{13}$$

Finally, $P(k, E_2)$ is the proton spectral function

$$P(k, E_2) = \frac{1}{(2\pi)^3}\frac{tM}{2}\frac{2}{\pi}\frac{1}{2}\sum_{\sigma_p\lambda}\sum_{j_f m_f S_f \mu}\left|\int \psi^{E_2 *}_{\lambda j_f m_f S_f}(\vec{r})\, e^{-i\vec{\rho}\cdot\vec{k}}\, \chi^{\sigma_p *}_{1/2}\, \psi^{\mu}_{1/2}(\vec{r}, \vec{\rho})\, d\vec{r}\, d\vec{\rho}\right|^2, \tag{14}$$

where $\vec{r}$ and $\vec{\rho}$ are Jacobian coordinates $\vec{r} = \vec{r}_1 - \vec{r}_2$, $\vec{\rho} = \vec{r}_3 - (\vec{r}_1 + \vec{r}_2)/2$, and λ labels the quantum number specifying the coupled states. The spectral function represents the probability distribution for finding in the triton the proton with momentum $\vec{k} = -\vec{k}_R$ and the neutrons with relative energy E_2. Inserting the triton wave function (3) in Eq. (14) one obtains

$$P(k, E_2) = \frac{1}{\pi^3}\frac{tM}{2}\sum_{\lambda S_f l_f}(2j_f + 1)\sum_{j l_b}(2j + 1)\left|\sum_{\substack{n_a n_b l_a \\ LS}} C_i \begin{Bmatrix} l_a & l_b & L \\ S_f & \frac{1}{2} & S \\ j_f & j & \frac{1}{2} \end{Bmatrix}(2L+1)^{1/2}(2S+1)^{1/2}\right.$$
$$\times \int_0^\infty u^{E_2 *}_{l_a S_f j_f \lambda}(\sqrt{2}\,a) R_{n_a l_a}(a)\frac{a}{\sqrt{2}}\,da$$
$$\left.\times \int_0^\infty j_{l_b}(kb/\sqrt{2}) R_{n_b l_b}(b) b^2 db\right|^2, \tag{15}$$

where R_{nl} is a radial harmonic oscillator wave function and $u^{E_2}_{l_a S_f j_f \lambda}(r)$ is the radial wave function describing the relative motion of the pair. As is well known, the spectral function is the central quantity which determines the electrodisintegration cross section for all possible coincidence and noncoincidence processes. A detailed study of the dependence of the spectral function upon the structure of the triton wave function and the two-neutron final-state interaction has been reported in Ref. 13. There it has been found that only the n-n final-state interaction in the $^1S_0$ wave has important effects on the spectral function which, moreover, is practically not affected by the components of the wave function with $l_a + l_b > 4$ [in the wave function (3) the values of l_a and l_b range up to 15]. Furthermore, it turns out that for any value of k, and $E_2 < 3$ MeV, and, on the other hand, for any value of E_2, and $k < 0.2$ fm^{-1}, the spectral function is essentially determined by the $l_a = l_b = 0$ components; in particular (see the continuous curves in Fig. 3), the sharp minima around 2.1 fm^{-1} for low values of E_2, and around 42 MeV for small values of k, are characteristic features of these components. The sensitivity of the spectral function upon the triton D-wave probability deserves particular attention. In Fig. 3 the spectral functions including all wave function components (full line)

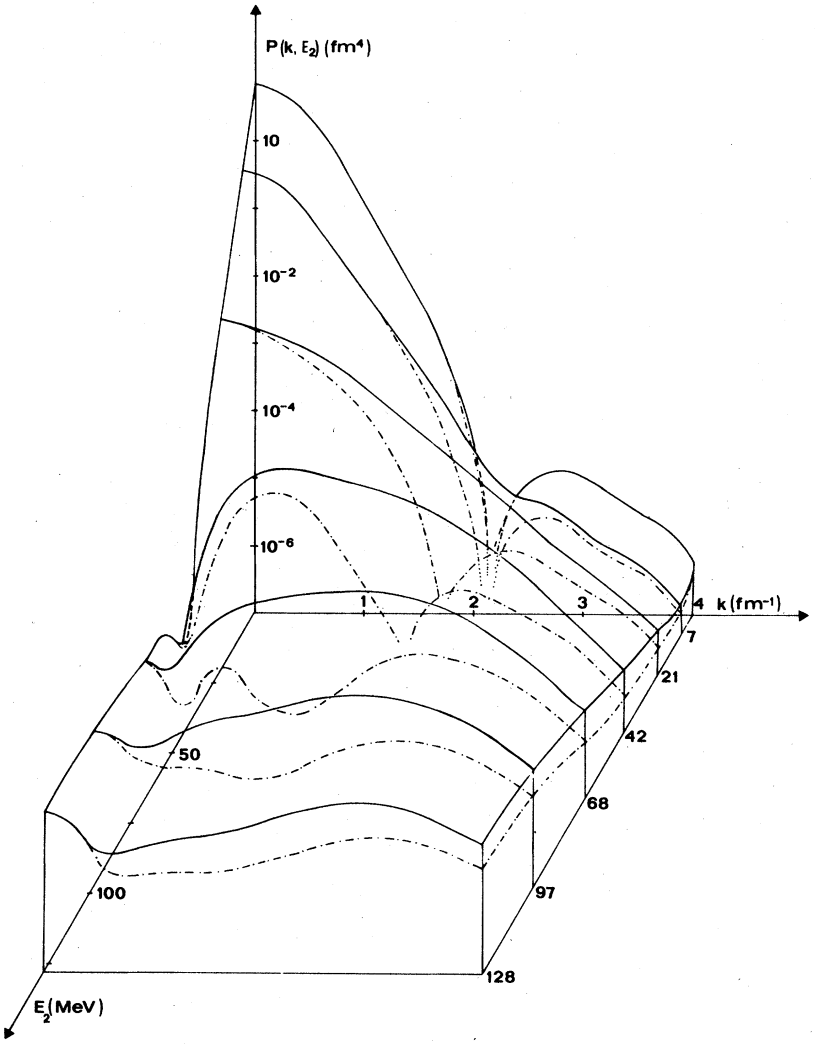

FIG. 3. Spectral function of the process $^3\mathrm{H}(e,e'p)2n$. The continuous lines represent the full calculation, whereas the dot-dashed lines correspond to the calculation performed omitting the triton $L=2$ wave.

and retaining only the $L=0$ component (dot-dashed line) are presented; substantial differences starting from $k\sim 1$ fm^{-1} are observed, even at low values of the two-neutron energy E_2. It can be noticed that the contribution from the D wave is very large; this fact casts several doubts on the validity (at $k\geq 1$ fm^{-1}) of calculations performed with wave functions containing only the $L=0$ component.

A more important question concerns the extent to which three-body wave functions featuring different D-wave percentages give rise to different spectral functions. In Fig. 4 the spectral functions corresponding to the RSC and RHEL-1 potentials are compared; it can be seen that the two spectral functions do differ. The problem as to whether this difference can be experimentally detected will be discussed in Sec. IV.

In Fig. 5 our spectral function and the one obtained by Dieperink *et al.*[12] using the Faddeev wave function of Ref. 1(a) are shown for $E_2=0.5$ MeV. It can be seen that the variational spectral function has a larger content of high momentum components; this feature is even more appreciable at higher values of E_2. It has recently been shown[22] that the larger momentum content of the variational wave function has important consequences in the calculation of various observables (see Sec. VII).

Finally, we would like to mention that the numerical accuracy of the calculation of our spectral function has been checked by computing, for each value of k, the momentum distribution in two different ways: (i) by using the expression $p(k)$

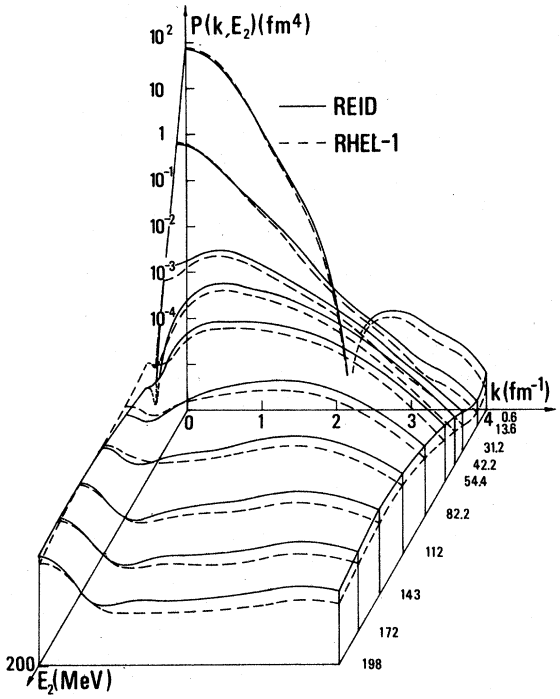

FIG. 4. Spectral function of the process $^3\mathrm{H}(e,e'p)2n$ calculated using the RSC interaction (continuous lines) and the RHEL-1 interaction (dashed lines).

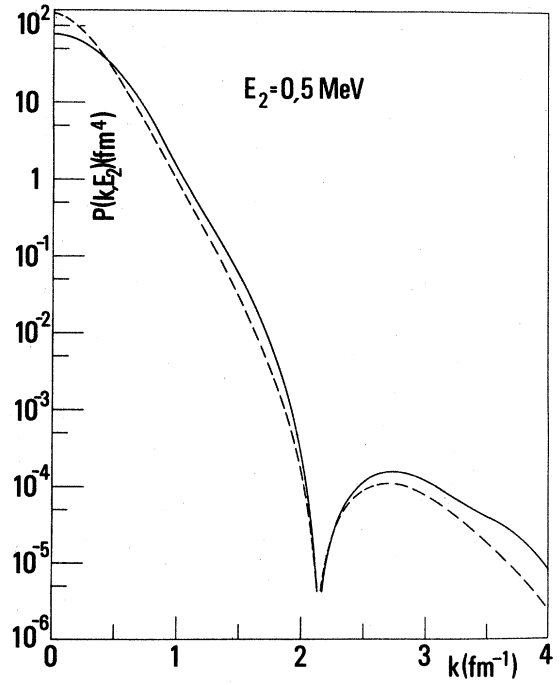

FIG. 5. Spectral function of the process $^3\mathrm{H}(e,e'p)2n$ calculated at $E_2 = 0.5$ MeV using the variational wave function [Ref. 4(a)] (continuous line) and the wave function of Ref. 1(a) [Ref. 21]. The interaction is the RSC potential.

$= \int_0^\infty P(k,E_2)dE_2$, (ii) directly from the wave function by means of a completely analytical calculation. The maximum difference between the two cases is less than one percent for every value of k.

IV. COINCIDENCE ANGULAR DISTRIBUTIONS FOR THE PROCESS $^3\mathrm{H}(e,e'p)2n$

The cross section for the coincidence process, the kinematics of which is depicted in Fig. 6, can be obtained by integrating Eq. (8) over the proton energy T_p and the relative energy E_2 obtaining

$$\frac{d^3\sigma}{d\Omega_2 d\epsilon_2 d\Omega_p} = \int_0^{E_2^{\max}} \frac{2k_p^2 M}{|3k_p - q\cos\varphi|}\left(\frac{d\sigma}{d\Omega}\right)_{ep} \times P(k,E_2)dE_2\,, \tag{16}$$

where the factor $2k_p/|3k_p - q\cos\varphi|$ is the recoil factor arising from the dependence of the energy conserving δ function upon k_p and

$$E_2^{\max} = \begin{cases} \omega - |E_3| - \dfrac{q^2}{12M}(3-\cos^2\varphi)\,, & |\varphi| \le \dfrac{\pi}{2} \quad (17) \\ \omega - |E_3| - \dfrac{q^2}{4M}\,, & |\varphi| > \dfrac{\pi}{2}\,. \quad (18) \end{cases}$$

Both k_p and k are functions of E_2 such that

$$k_p = \tfrac{1}{3}q\cos\varphi + \tfrac{1}{3}\left[q^2\cos^2\varphi - 12M \times\left(E_2 + |E_3| - \omega + \frac{q^2}{4M}\right)\right]^{1/2}, \tag{19}$$

$$k = [4M(\omega - |E_3| - E_2) - 2k_p^2]^{1/2}. \tag{20}$$

We neglect the other value of k_p, with a minus sign in front of the square root, since its contribution is negligible in the kinematical region we have chosen which corresponds to the experimental conditions by Johansson,[23] that is, $\epsilon_1 = 550$ MeV, $\epsilon_2 = 441$ MeV, $\theta_e = 51.7°$, $\theta_p = 44.2$, 51.5, and 62°, so that $\omega = 109$ MeV and $q = 2.2$ fm^{-1}.

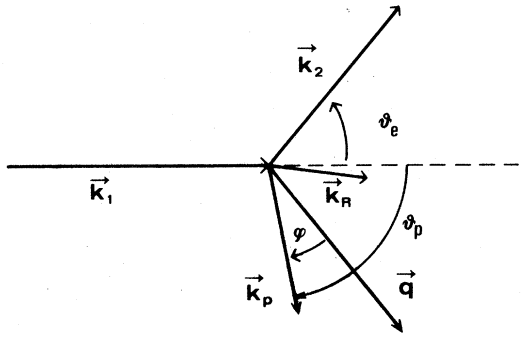

FIG. 6. Kinematics of the reaction $^3\mathrm{H}(e,e'p)2n$ (note that in Ref. 13, θ_p denotes the angle between $\vec{k}_p$ and $\vec{q}$).

It should be pointed out that in the three-body electrodisintegration there is no one-to-one correspondence between the values of the proton emission angle φ and the proton internal momentum k, since for a fixed value of φ, due to the variation of E_2 in Eq. (16), $0 \leq E_2 \leq E_2^{\max}$, the value of k_p varies from $k_{p_{\max}}$ to $k_{p_{\min}}$ and correspondingly, k varies from $k_{\min}$ to $k_{\max}$. However, it has been shown[13] that the function $k = k(E_2)$ plotted for various values of φ exhibits almost a constant behavior for not too large values of the energy (except for small φ); since the spectral function for low values of k drops out very rapidly as a function of E_2, in the range $11° < |\varphi| < 61°$ there is actually a very small contribution to the cross section (16) from the values of E_2 such that $k(E_2)$ is different from a constant. It turns out, therefore, that as far as the cross section (16) is concerned, to each value of φ in the above range corresponds a unique value of k, and vice versa. If the kinematical conditions are varied so as to increase the energy and momentum transfer (for example, $\omega = 140$ MeV, $q = 2.45$ fm^{-1}) the function $k = k(E_2)$ becomes constant on a larger energy range. Then the experimental measurement of the proton momentum distribution from the experimental cross section $d^4\sigma/d\epsilon_2 d\Omega_2 dT_p d\Omega_p$, at a fixed value of φ, would be possible in the range of k from 0.5 to 1.8 fm^{-1}. Indeed, for each φ, the function $k(E_2)$ is a constant in the energy interval $(0, E_2')$; the momentum distribution is given by

$$p(k) = \int_0^\infty dE_2 P(k, E_2) , \tag{21}$$

but, due to the rapid drop out of $P(k, E_2)$, one can write

$$p(k) \sim \int_0^{E_2'} dE_2 P(k, E_2) \cong \int_0^{E_2'} dE_2 \frac{1}{(d\sigma/d\Omega)_{ep} Mk_p} \left(\frac{d^4\sigma}{d\epsilon_2 d\Omega_2 dT_p d\Omega_p} \right) \Big|_{\varphi = \varphi(k)} . \tag{22}$$

The coincidence cross section [Eq. (16)] computed from the wave function (3), both including and omitting the triton D wave and disregarding in Eq. (11) the convection current terms (which yield a very small contribution), is shown in Fig. 7 together with the experimental data of Johansson.[23] It can be seen that the angular distributions corresponding to different nucleon-nucleon interactions do differ at high proton scattering angles by about 30% and this difference can be almost entirely ascribed to the difference in the D wave percentages.

A careful check, for each value of φ, of the convergence of the angular distributions with the maximum number $Q_{\max}$ of oscillator quanta included in the basis, has been performed. A very good convergence of the theoretical angular distributions is obtained for $|\varphi| > 10°$. The convergence, however, is not very good at lower angles; this means that the theoretical results strongly depend upon $Q_{\max}$, so that the computed angular distributions have to be extrapolated to higher values of $Q_{\max}$; the extrapolation procedure leads to an uncertainty in the theoretical results, represented in Fig. 7 by the shaded area at low scattering angles. The results presented in Fig. 7 clearly show that the variational wave function of Ref. 4 is not the best suited for the calculation of the angular distributions at low values of φ (or k). This is due to the fact that the low momentum part of the angular distributions does depend upon the asymptotic part of the wave function which has not yet converged at $Q_{\max} = 28$. However, at higher values of k, where the asymptotic part of the wave function does not play any significant role, the convergence of the angular distributions is very good.

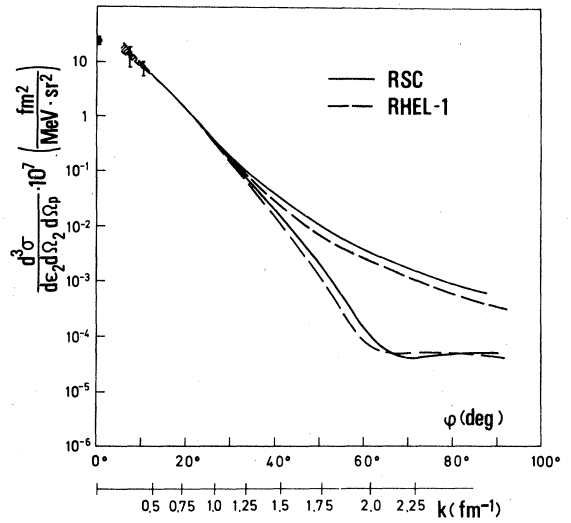

FIG. 7. Angular distributions of the reaction ^{3}H$(e, e'p)2n$. In the upper curves all wave function components are present, whereas in the lower curves the triton D wave is omitted. The experimental data are from Ref. 23. For the meaning of the shaded area, see text.

Fabian and Arenhoevel[24] have shown that the effects of meson exchange currents (MEC) and isobar configurations on the reaction $d(e, e'p)n$ in the quasi-elastic region are small; one expects that these effects will be small also on the reaction ^{3}H$(e, e'p)2n$. Therefore, the measurement of the angular distributions of this reaction may provide useful information on the S- and D-wave momentum distributions.

It should be pointed out that coincidence reac-

tions in the quasi-elastic region have several advantages with respect to the elastic electron scattering because: (i) although the charge form factor of ^{3}He does depend upon the D wave percentage, it is not possible to obtain reliable information on the D-wave percentage due to the uncertainties in the knowledge of the nucleon charge form factor and in the theoretical treatment of MEC and relativistic effects[16]; (ii) as is well known, the details of the wave function, which appear in the momentum distribution at a momentum k, appear in the charge form factor at a momentum transfer q considerably larger than k (see, e.g., Ref. 25), so that a nonrelativistic description of the charge form factor may not be valid; (iii) at $k \geq 1.3$ fm^{-1} the angular distributions are entirely determined by the D wave, whereas in the charge form factor the contributions from the S and D waves overlap in the full range of momentum transfer.

V. THE QUASI-ELASTIC PEAK IN ELECTRON-TRITON SCATTERING

The quasi-elastic peak in electron-triton scattering is given by the incoherent sum of the following processes:

$$e + {}^3\mathrm{H} \rightarrow e' + p + (nn)\,, \tag{23a}$$

$$e + {}^3\mathrm{H} \rightarrow e' + n + d\,, \tag{23b}$$

$$e + {}^3\mathrm{H} \rightarrow e' + n + (np)\,. \tag{23c}$$

As shown by Lehman,[19] the main contribution to the quasi-elastic peak comes from the three-body disintegration (23a). This process is the simplest one to calculate with wave functions of the type (3). In fact, the calculation of processes (23b) and (23c) and, more generally, the calculation of all those processes characterized by a two-nucleon final state composed by the two unlike particles, e.g., ^{3}He$(e,e'p)d$ or ^{3}He$(e,e'p)np$, is more complicated. The difficulties arise from the fact that since in Ref. 4 the isotopic spin formalism has not been used, a change of variables from $\vec{a}$ and $\vec{b}$ to $\vec{r} = \vec{r}_1 - \vec{r}_3$ and $\vec{\rho} = \vec{r}_2 - \frac{1}{2}(\vec{r}_1 + \vec{r}_3)$ (1 and 2 label the like particles) and the corresponding recoupling of the angular momenta are necessary in order to compute the processes (23b) and (23c). This can be accomplished only by introducing the generalized Moshinsky brackets,[26] which lead to a very complicated expression for the cross section; the evaluation of this cross section represents therefore a cumbersome computational task, without involving, however, any difficulty of theoretical character. In this paper, only the results for process (23a) will be presented, whereas the results including the other two processes will be presented elsewhere. It is clear that having calculated only process (23a), any comparison with the experimental data is meaningless.

Integrating the cross section (8) over the variables T_p, Ω_p, and E_2 one gets

$$\frac{d^2\sigma}{d\epsilon_2 d\Omega_2} = \left(\frac{d\sigma}{d\Omega}\right)_{ep} \int_0^{E_2^{\max}} dE_2 \int_{k_{\min}}^{k_{\max}} dk P(k, E_2) 2\pi \frac{Mk}{q}\,, \tag{24}$$

where

$$E_2^{\max} = \omega - |E_3| - \frac{q^2}{6M}\,, \tag{25}$$

and

$$k_{\min} = \left|\tfrac{2}{3}q - k_0\right|\,, \tag{26}$$

$$k_{\max} = \tfrac{2}{3}q + k_0\,, \tag{27}$$

with k_0 being the relative momentum between the proton and the neutron pair

$$k_0 = \left[\frac{4M}{3}\left(\omega - |E_3| - \frac{q^2}{6M} - E_2\right)\right]^{1/2}. \tag{28}$$

The calculated quasi-elastic peak corresponding to the kinematical conditions by Hughes *et al.*[27] is shown in Fig. 8. As previously explained, the

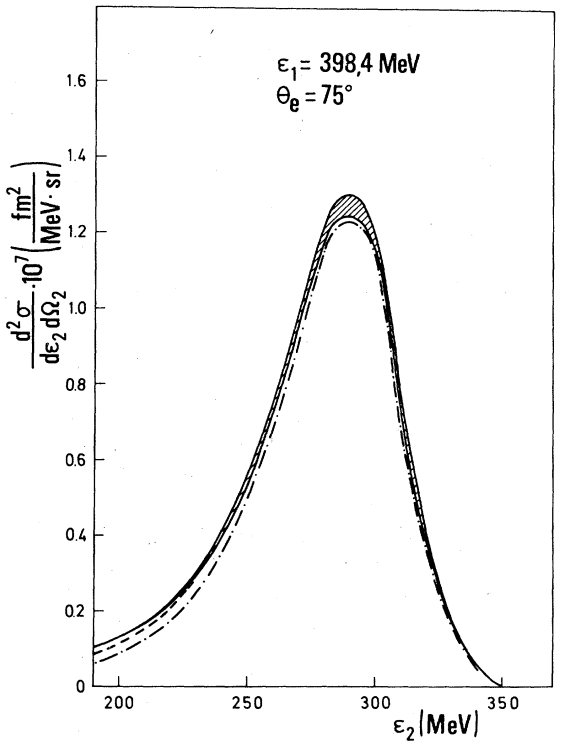

FIG. 8. The quasi-elastic peak corresponding to the process ^{3}H$(e,e'p)2n$. The dot-dashed line has been obtained using the RSC potential and omitting the triton D wave, whereas the full line corresponds to the case wherein all wave function components are retained. The dashed line corresponds to the RHEL-1 potential including all wave function components.

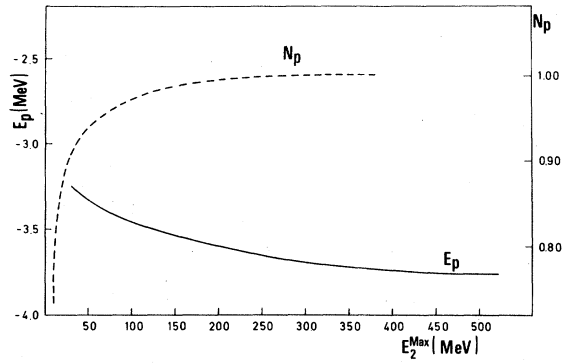

FIG. 9. Proton number N_p and proton energy per particle E_p calculated from Eqs. (32) and (29) as a function of the upper limits of integration $E_2^{\max}$ and $k_{\max} = (4ME_2^{\max})^{1/2}$ using the RSC interaction.

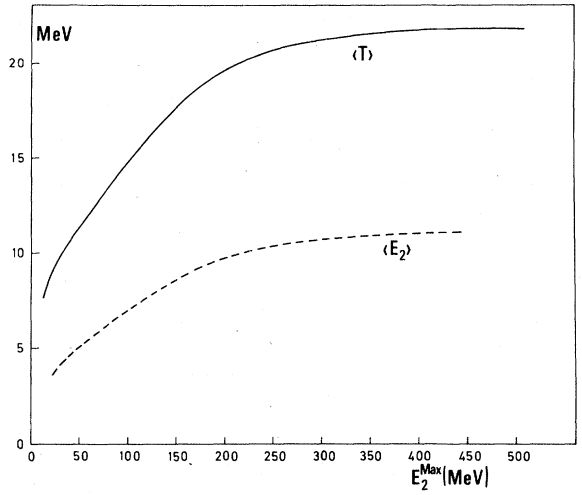

FIG. 10. The same as in Fig. 9 for the proton mean kinetic energy $\langle T\rangle$ [Eq. (30)] and the mean n-n excitation energy $\langle E_2\rangle$ [Eq. (31)].

thickness of the curve, which reflects the uncertainty of the calculation due to the extrapolation procedure, has to be ascribed to the dependence of the top of the peak upon the nonconverging (at $Q_{\max} = 28$) asymptotic part of the wave function.

Dieperink *et al.*[12] argued that the wave function components with high values of angular momenta might help in removing the discrepancy between theory and experiment in the quasi-elastic peak of ^{3}He at a transferred energy $\omega > 150$ MeV. We have, on the contrary, found that, at least for the process we have considered, neglecting the components $l_a + l_b > 4$ has no influence at all on the quasi-elastic peak, the high energy tail of which is instead affected by the D wave as shown in Fig. 8. It should be pointed out that the kinematical conditions by Hughes *et al.* used to obtain the curves shown in Fig. 8 are not the best suited in order to display the effect from the triton D wave. For example, if $\theta_e = 65°$ instead of 75° is used, our spectral function will lead to a large contribution from the D wave already at $\omega = 160$ MeV. A detailed study of the effect of the triton D wave in the quasi-elastic peak is under way and will be reported elsewhere. From the results presented in this paper, it appears, however, that some doubts might be raised against calculations of the quasi-elastic peak in heavier nuclei based on simple S-wave wave functions.

VI. THE ENERGY-WEIGHTED SUM RULE

The energy-weighted sum rule,[15] which expresses the energy per proton E_Z/Z through the proton mean removal energy $\langle E\rangle = \langle E_2\rangle + |E_3|$ and the mean kinetic energy $\langle T\rangle$, reads in our case

$$E_p = \tfrac{1}{2}(\tfrac{1}{2}\langle T\rangle - \langle E_2\rangle) + \tfrac{1}{2}E_3 , \qquad (29)$$

where

$$\langle T\rangle = \frac{4\pi}{N_p}\int_0^\infty\int_0^\infty P(k,E_2)\frac{k^2}{2M}k^2dk\,dE_2 , \qquad (30)$$

$$\langle E_2\rangle = \frac{4\pi}{N_p}\int_0^\infty\int_0^\infty P(k,E_2)E_2k^2dk\,dE_2 , \qquad (31)$$

$$N_p = 4\pi\int_0^\infty\int_0^\infty P(k,E_2)k^2dk\,dE_2 . \qquad (32)$$

The quantities $\langle T\rangle$, $\langle E_2\rangle$, and N_p have been calculated as a function of the upper limits of integration $E_2^{\max}$ and $k^{\max} = (4ME_2^{\max})^{1/2}$. Their behavior is shown in Figs. 9 and 10. The asymptotic values are $\langle T\rangle = 21.76$ MeV, $\langle E_2\rangle = 11.10$ MeV, and $N_p = 1$, so that, using in Eq. (29) the calculated value $E_3 = -7.3$ MeV, one gets for the proton energy $E_p = -3.76$ MeV. The neutron energy per particle is $E_n = \frac{1}{2}(E_3 - E_p) = -1.77$ MeV. The difference between E_p and E_n is due to the different interaction acting in the p-n and n-n pairs. Neglecting the Coulomb interaction, one obtains $E_n(^3\text{He}) = E_p(^3\text{H}) = -3.76$ MeV and $E_p(^3\text{He}) = E_n(^3\text{H}) = -1.77$ MeV. The various energies obtained from Eqs. (29), (30), and (31) are collected in Table II.

TABLE II. Calculated binding energy E_3, mean proton kinetic energy $\langle T\rangle$ [Eq. (30)], mean excitation energy of the n-n pair $\langle E_2\rangle$ [Eq. (31)], and mean proton removal energy $\langle E\rangle = |E_3| + \langle E_2\rangle$; E_p and E_n are the proton and neutron energy per particle calculated from Eq. (29). The nucleus is ^{3}H and the interaction the RSC potential. All quantities are in MeV.

E_3	$\langle T\rangle$	$\langle E_2\rangle$	$\langle E\rangle$	E_p	E_n
−7.3	21.76	11.1	18.4	−3.76	−1.77

The results presented in Fig. 9 allow us to estimate the maximum value of the experimental removal energy $E^{\max} = |E_3| + E_2^{\max}$ which has to be reached in order to measure the value of E_p with a given precision. For example, if a precision of 10% is required, the value $E_2^{\max} \sim 70$ MeV ($k^{\max} \sim 2.6$ fm^{-1}) has to be reached; correspondingly, the value of N_p can be measured with a precision of about 4.5%. From Fig. 10 it can be seen that $\langle T \rangle$ and $\langle E_2 \rangle$ saturate very slowly. In fact, for $E_2^{\max} \sim 70$ MeV, $\langle T \rangle$ is only 59% of the asymptotic value and $\langle E_2 \rangle$ only 49.5%. However, in Eq. (29) $\frac{1}{2}\langle T \rangle$ and $\langle E_2 \rangle$ are almost of the same order and this gives rise to the rapid saturation of E_p.

VII. DISCUSSION AND CONCLUSIONS

The following results of the calculations presented in this paper are worth being mentioned: (1) It has been found that a difference in the D-wave probability in ^{3}H, resulting from different two-body interactions, might in principle be detected by a precise coincidence experiment even at not very large values of the proton momentum ($k \sim 1.5$ fm^{-1}). (2) The variational wave function of Ref. 4(a) leads to a spectral function for the processes $^3\mathrm{H}(e,e'p)2n$ and $^3\mathrm{He}(e,e'n)2p$, different from the spectral function obtained in Ref. 21 using the wave function of Ref. 1(a) in that it contains a larger amount of high momentum components. For this reason we believe that the discrepancies between the theoretical calculations and the experimental data of the quasi-elastic peak of ^{3}He found in Ref. 12 might be partly removed by using the variational wave function of Ref. 4(a). The calculation[22] of the $T=1$ contribution to the high energy tail for ^{3}He using the kinematics of Ref. 28 shows indeed that the high momentum components, which are present in the variational wave function, produce a tail higher by about a factor of 2 than the corresponding tail obtained with the Faddeev wave function of Ref. 1(a). Since the tail of the quasi-elastic peak converges very well (see, e.g., Fig. 8 and Ref. 22), the difference in the high momentum content between the two wave functions is a real and a detectable one.

The fact that the variational wave function of Ref. 4(a) has more high momentum components than the wave function of Ref. 1(a) obviously does not indicated a superiority of the variational method. It simply indicates that the two wave functions are not fully equivalent. We would like to mention only two possible reasons for such nonequivalence: (i) The cutoff in momentum which is necessary in order to solve the Faddeev equations may, in principle, affect the momentum content of the wave function. (ii) The two-body interaction used in Refs. 4(a) and 1(a) is not completely equivalent; in the former all waves with $j \leq 2$ were considered, whereas in the latter only the waves $^1S_0$, $^3S_1$-$^3D_1$ were included in the calculation. The effect on the charge form factor of the momentum cutoff has been carefully investigated in Ref. 1(a); moreover, the charge form factors calculated by solving the Faddeev equations in momentum[1(a)] and coordinate[2] spaces are almost identical. For these reasons we are tempted to conclude that the lack of the P wave interaction in the calculations performed in Ref. 1(a) might be the origin of the different momentum content of the two wave functions that we have considered (the importance of the odd state interaction in the computation of the charge form factor has been shown by Strayer and Sauer[3]).

The feature of our calculations which deserves further improvement concerns the treatment of the final-state interaction between the proton and the n-n pair, which is completely neglected in the PWA. The latter is the more valid the higher the kinetic energy of the emitted proton and the lower the relative energy of the n-n pair. The kinetic energy of the proton relative to the n-n pair is

$$T_0 = \omega - |E_3| - \frac{q^2}{6M} - E_2 . \tag{33}$$

For the kinematical conditions of the coincidence experiment by Johansson, at proton angles $|\varphi| < 25°$, the contribution to the cross section resulting from $E_2 > 10$ MeV is negligible, $T_0 \sim 60$ MeV and the PWA can probably be considered accurate enough. However, to have more confidence in the validity of the PWA, both at low and high scattering angles, future experiments should be performed at higher values of the energy transfer ω, so as to have much larger values of T_0.

A consistent treatment of the final-state interaction in the processes $^3\mathrm{He}(\gamma,p)d$, $^3\mathrm{He}(\gamma,p)np$, and $^3\mathrm{He}(e,e'p)d$ has been performed by means of the Faddeev formalism and the hyperspherical harmonics method.[29] The price one has to pay for these thorough calculations of the final-state interaction is the use of simple separable S-wave interactions which might even provide a good explanation of the existing low momentum angular distributions (see, e.g., Ref. 29c), but which becomes inadequate at high values of k (see, e.g., Fig. 7). In light of the planned new generation of quasi-elastic electron scattering experiments on the few-body systems,[25] aimed at the study of the high (k, E_2) part of the spectral function, the calculation of this quantity with realistic nucleon-nucleon interactions becomes a prerequisite for a meaningful comparison between theoretical calculations and experimental data.

ACKNOWLEDGMENTS

During the early stage of this work we have benefitted from several discussions with various people, particularly with Y. E. Kim and I. Sick. We are indebted to A. E. L. Dieperink for supplying the spectral function calculated with the Faddeev wave function.

[1](a) R. A. Brandenburg, Y. E. Kim, and A. Tubis, Phys. Rev. C 12, 1368 (1975); (b) E. P. Harper, Y. E. Kim, and A. Tubis, Phys. Rev. Lett. 28, 1533 (1972); (c) Phys. Rev. C 2, 877 (1970); C 6, 126 (1972). The wave function used in Ref. 1(a) is an improved version of the wave function of Ref. 1(b), in that the momentum cutoff q_{max} was extended from 1.7 to 3.1 fm^{-1}.

[2]A. Laverne and G. Gignoux, Phys. Rev. Lett. 29, 436 (1972); Nucl. Phys. A203, 597 (1973).

[3]M. R. Strayer and P. U. Sauer, Nucl. Phys. A231, 1 (1974).

[4](a) P. Nunberg, E. Pace, and D. Prosperi, Nucl. Phys. A285, 58 (1977); (b) P. Nunberg, D. Prosperi, and E. Pace, Lett. Nuovo Cimento 17, 76 (1976).

[5]V. F. Demin, Yu. E. Pokrovsky, and V. D. Efros, Phys. Lett. 44B, 227 (1973); V. F. Demin and Yu. E. Pokrovsky, Phys. Lett. 47B, 394 (1973).

[6]Y. E. Kim and A. Tubis, Ann. Rev. Nucl. Sci. 24, 69 (1974).

[7]P. Nunberg, D. Prosperi, and E. Pace, in *The Nuclear Many Body Problem*, edited by F. Calogero and C. Ciofi degli Atti (Editrice Compositori, Bologna, 1973), Vol. I, p. 215.

[8]C. Ciofi degli Atti, in *Lecture Notes in Physics*, edited by S. Costa and C. Schaerf (Springer, Berlin, 1977), Vol. 61, p. 521.

[9]A. C. Phillips, Rep. Prog. Phys. 40, 905 (1977).

[10]B. A. Craver, Y. E. Kim, and A. Tubis, Nucl. Phys. A276, 237 (1977).

[11]R. V. Reid, Jr., Ann. Phys. (N.Y.) 50, 411 (1968).

[12]A. E. L. Dieperink, T. de Forest, I. Sick, and R. A. Brandenburg, Phys. Lett. 63B, 261 (1976).

[13]C. Ciofi degli Atti, E. Pace, and G. Salmè, in *Lecture Notes in Physics*, edited by C. Ciofi degli Atti and E. De Sanctis (Springer, Berlin, 1978), Vol. 86, p. 316.

[14]I. Ulehla, in *The Nuclear Many Body Problem*, edited by F. Calogero and C. Ciofi degli Atti (Editrice Compositori, Bologna, 1973), Vol. I, p. 145.

[15]S. Boffi, Lett. Nuovo Cimento 1, 931 (1971); D. S. Koltun, Phys. Rev. Lett. 28, 182 (1972).

[16]C. Ciofi degli Atti, E. Pace, and G. Salmè, in lectures delivered at the International School of Intermediate Energy Nuclear Physics, Ariccia, Italy, 1979, *Surveys in High Energy Physics* (Harwood Academic, London, to be published); E. Pace, Lett. Nuovo Cimento (to be published).

[17]E. Pace, P. Nunberg, and D. Prosperi, in *Lecture Notes in Physics*, edited by C. Ciofi degli Atti and E. De Sanctis (Springer, Berlin, 1978), Vol. 86, p. 256.

[18]I. Sick, in *Lecture Notes in Physics*, edited by C. Ciofi degli Atti and E. De Sanctis (Springer, Berlin, 1978), Vol. 86, p. 299.

[19]D. R. Lehman, Phys. Rev. C 3, 1827 (1971).

[20]C. Ciofi degli Atti, *Progress in Particle and Nuclear Physics*, edited by D. Wilkinson (Pergamon, New York, to be published).

[21]A. E. L. Dieperink (private communication).

[22]C. Ciofi degli Atti, E. Pace, and G. Salmè, invited paper to the Conference Nuclear Physics with Electromagnetic Interactions, Mainz (FRG), 1979, in *Lecture Notes in Physics*, edited by H. Arenhoevel and D. Drechsel (Springer, Berlin, 1979), Vol. 108, p. 412.

[23]A. Johansson, Phys. Rev. 136, B1030 (1964).

[24]W. Fabian and H. Arenhoevel, Nucl. Phys. A314, 253 (1979).

[25]J. Mougey, in *Lecture Notes in Physics*, edited by C. Ciofi degli Atti and E. De Sanctis (Springer, Berlin, 1978), Vol. 86, p. 304.

[26]Yu. F. Smirnov, Nucl. Phys. 27, 177 (1961); 39, 346 (1962).

[27]E. B. Hughes, T. A. Griffy, M. R. Yearian, and R. Hofstadter, Phys. Rev. 139, B458 (1965).

[28]J. S. McCarthy *et al.*, Phys. Rev. C 13, 712 (1976).

[29](a) B. F. Gibson and D. R. Lehman, Phys. Rev. C 11, 29 (1975); C 13, 477 (1976); (b) V. K. Tartakovskiĭ, Yad. Fiz. 20, 46 (1974) [Sov. J. Nucl. Phys. 20, 23 (1975)]; (c) C. R. Heibach, D. R. Lehman, and J. S. O'Connell, Phys. Lett. 66B, 1 (1977).